

INVERTED CURVED FLEXURE HINGE WITH TORSIONAL REINFORCEMENTS IN A PRINTED PROSTHETIC FINGER

A.S. (Bas) Boers, M. (Mark) Naves,
L.A. (Luis) Garcia Rodriguez, D.M. (Dannis) Brouwer
Precision Engineering lab
University of Twente
The Netherlands

ABSTRACT

Flexure-based finger joints for prosthetic hands have been studied, but until now they lack stiffness and load capacity. In this paper we present a design which combines large range of motion, stiffness and load capacity, with a torsional overload protection mechanism. Five design considerations which increase grasp force and limit the stress values are presented: (1) Due to the inverted flexure attachment, the flexures are loaded mainly in tension, avoiding buckling of flexures. (2) Curved flexures have been used of which one straightens out at large deflection angles to improve load capacity at large deflections. (3) To achieve high torsional loads, one of the flexures is outfitted with triangular torsional stiffeners, which increase the out-of-plane stiffness significantly, while only slightly increasing the actuation stiffness. (4) The entire joint is rotated by 20° so the combination of actuation and contact forces lead to mainly axial forces in the curved leaf spring, avoiding excessive internal bending.

The presented prosthetic flexure-based finger joint is able to achieve 20N of contact force with an additional 5N of out of plane load over the entire 80° range of motion, which is a major improvement over existing prosthetic flexure-based finger designs.

INTRODUCTION

Flexure joints applied in prosthetic and robotic hands have been of interest in recent years [1–4]. The main advantages for prosthetic hands are lightweight design, (almost) no assembly needed, reduced cost, and precise grasping force without force feedback. [3–5].

A major challenge for flexure joints in large range of motion applications is the strong decrease of support stiffness in load carrying directions when deflected [6–8]. This loss of support stiffness and accompanying poor load carrying capacity at large rotations currently prevents widespread applicability in robotic and prosthetic hands [3]. Therefore, it is of interest to

study the mechanical behavior of monolithic integrated flexure joint designs over the entire range of motion. The decrement of the stiffness in the support direction also leads to loss of load bearing capacity of the hand. Especially when including tendon actuation and high grasping forces, elastic instability of the joint (buckling) can result in reduced load-carrying capacity.

Researchers from the UB Hand compared several flexure topologies for robotic hands by analyzing compliance matrices in undeflected position [4],[9]. Additionally, Tavakoli et al. presented new topologies and analyzed the flexure stresses and deflections for the undeflected state [1]. Although analyzing the stiffness properties of flexure topologies at undeflected state allows the use of simple linear beam equations, it gives no lead to the stiffness properties at larger deflection angles due to the strong non-linear behavior. Furthermore, as critical stiffness and load carrying capacity typically occurs at maximum deflection, the mechanical properties at maximum deflection angle is of primary interest rather than at the undeflected state.

Kalpathy used a pseudo-rigid-body model with an approximation of Timoshenko beam theory to model leafsprings in a larger range of motion [2]. Although pseudo rigidbody modeling allows for larger deflections, it is limited to simulation of its kinematic behavior and stiffness in the free motion direction. Therefore, evaluation of the support stiffness at large deflection angles is still unavailable.

Odhner presented the “Smooth Curvature model” to calculate compliance matrices in large deflections of planar leafspring designs, as this can be associated with stable grasps [10]. This method allows for evaluation of support stiffness at larger deflections, however, it described the compliance matrix only for the 2-dimensional case. For typical loading-conditions, out-of-plane stiffness and load carrying capacity are important also. Furthermore, it only allows for the evaluation of planar hinge designs.

In this study, a finger is investigated with two finger joints, the MCP (metacarpophalangeal) and PIP (proximal interphalangeal) joint. The DIP (distal interphalangeal) joint is considered rigid. The main focus will be on the design of the PIP joint, which is located in the middle of the finger and is more limited with the available space than the MCP joint. However, the general design considerations still apply to the MCP joint. In Figure 1, the basic geometry of the proposed prosthetic finger is shown, consisting of two joints with two crossing leaf springs each.

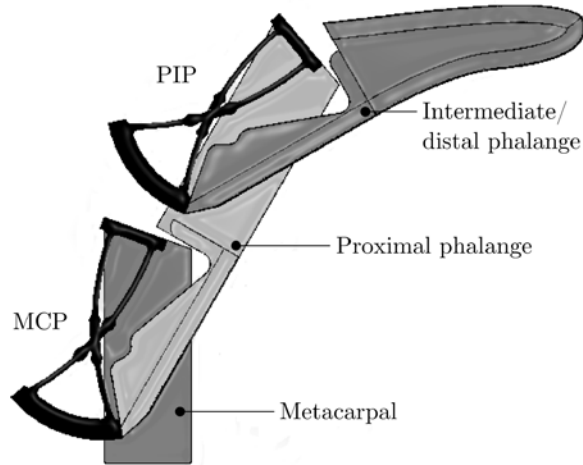


FIGURE 1. Schematic overview of finger design.

Since the working space is limited, an actuation moment cannot be achieved by placing rotational motors in the finger. Therefore, tendons are usually fitted inside the finger, as is the case in a human hand. This tendon only creates flexion (grasping action) of the finger. Extension can be achieved, but only if the finger is pressed against other objects.

REQUIREMENTS

The cylindrical medium power wrap is identified as one of the most commonly used grasps [11], [12] and therefore the main focus of this research. First of all, the flexure joint has to be able to withstand the actuation forces to achieve the required deflection of $\pm 40^\circ$. Additionally, the finger has to be able to create a contact force F_c acting on the inside of the finger resulting from the medium power wrap, which will have a large contribution to the actuation force. Contact forces in humans can reach up to 60N per finger when evaluating the contact force at a distance of 20 mm from the center of rotation of a human finger joint [13].

In this study, the goal is to design a finger for a hand which allows the user to hold a 2.5kg bottle. When the load is distributed over 5 contact points (four fingers and a thumb), the resulting out-of-plane load (F_s) is approximately 5N per finger. This load combined with an estimated friction coefficient of 0.2 results in a required grasping force (F_c) of approximately 20N. A schematic illustration of the resulting forces when holding a 2.5kg bottle is provided in Figure 2, in which F_a represents the actuation force provided by the tendon. In Table 1 a summary of the requirements is provided.

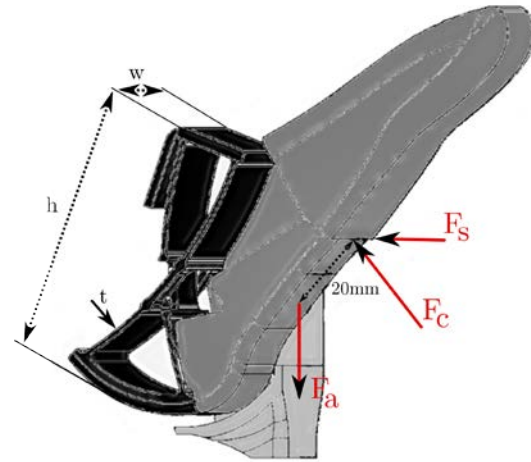


FIGURE 2. Schematic overview of forces acting on the PIP joint with $w=15\text{mm}$ and $h=40\text{mm}$. Note: the gravity direction is in the direction of force F_s .

TABLE 1: Boundary conditions

Parameters	Boundary conditions
Joint Height (h)	< 40 mm
Joint width (w)	< 15 mm
Flexure thickness (t)	> 0.8 mm (limit AM)
Deflection angle (θ)	$\pm 40^\circ$
Out-of-plane load (F_s)	5N
Contact Force (F_c)	To be maximized
Material	Nylon (PA2200)
Allowable stress	40 MPa
Flexural modulus	1.5 GPa

METHOD

Structural simulations are carried out to investigate the behavior of the finger joint for different load cases. For this simulation, an out-of-plane load (F_s) of 5 N and an contact force (F_c) of 20N is applied to the finger as illustrated in figure 2. Furthermore, action force (F_a) is altered in order to obtain static equilibrium over a

range of motion $-40^\circ < \theta < +40^\circ$. Simulations are conducted with the flexible multibody program SPACAR which uses a series of interconnected nonlinear 3D finite beam elements which includes geometric nonlinearities [14]. Additionally, the results are verified with finite element simulations in SolidWorks.

With the use of these simulations, the shape of the flexures is altered (the values of w, h and t) and the influence of the design considerations described in the next section is analyzed.

DESIGN AND MODELLING

Inverted mounting of the leaf springs

In order to achieve the required high contact and grasping forces, significant actuation forces are required. In its simplest implementation of a cross flexure actuated by a tendon, the leaf springs are loaded in compression. This concept is illustrated in Figure 3. Loading the leaves in compression severely limits the maximum actuation forces, and therefore the contact forces, because of buckling. Especially at large deflection angles, the leaves will be curved and the resistance to buckling will diminish.

A solution is to mount the leaves at the top of the phalanx, such that the leaves are loaded in tension. This creates an 'inverted joint', which is also shown in the finger design in Figure 1.

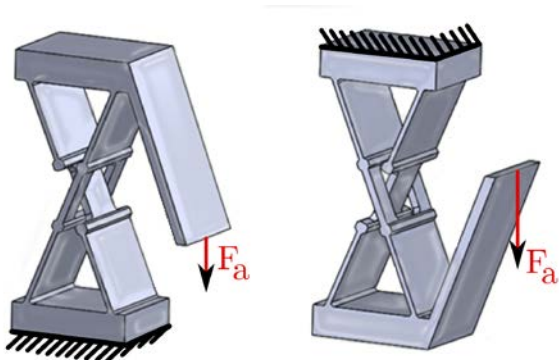


FIGURE 3. Crosshinge loaded in compression and prone to buckle (left), crosshinge loaded in tension due to inversion (right)

Curved Leaf Springs

The curvature of the leaf springs in traditional cross flexures increases as the deflection angle increases. Due to the fact that the maximum loading condition typically occurs at large deflection angles (i.e. a closed hand due to the

grasping operation), the highest forces occur when support stiffness and load carrying capacity is at their lowest. In order to compensate for this effect, two flexures which are equally curved and mirrored with respect to each other are used. This way, one of the leaves straightens out in either direction of motion providing high load capacity and support stiffness at larger deflection angles. A schematic illustration is provided in figure 4.

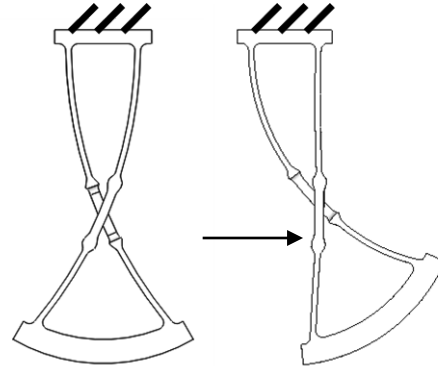


FIGURE 4. Curved Cross Hinge; deflection will result in one of the leafs straightening out.

The joint design is similar to the Curved Hinge presented in [15]. However, due to the possibilities of 3D printing, two crossing leaves can be fabricated. The stiffness of the curved leaf in the direction of the actuation force will be small with respect to the stiffness of the straightened leaf spring. Therefore, the majority of the forces will be fed through the straight leaf, as the leaves are connected in parallel. This means that the strongest leaf is loaded the heaviest, avoiding unwanted stress concentrations in the strongly curved leaf.

A comparison of the stress between a traditional Cross hinge and a Curved Cross Hinge is given 5N of sideways force (F_s) and 20N of contact force (F_c) is presented in figure 5. For the Cross Flexure, the stress at 0° (neutral position) when loaded with 20N starts out low (Figure 10). As the deflection angle increases, the stress increases due to both bending and additional internal moments caused by the deflected state of the flexures combined with the external load of 20N. Therefore, stress increases strongly with increasing deflection angle.

For the Curved Cross Hinge the situation is different. At the neutral state, the leaves are curved and therefore initially higher internal moments are present in the flexures, causing

higher stress levels. As the deflection angle increases, bending of the flexures results in an increase of stress. However, as the curvature of the flexure reduces, the internal moments caused by the external load decreases. The combined effect is a rather constant stress profile over the range of motion.

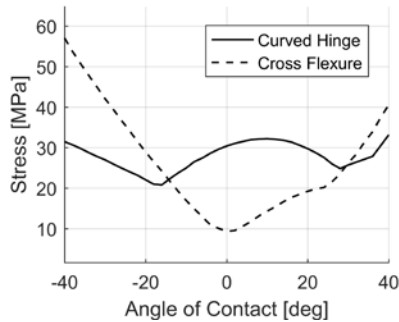


Figure 5: SPACAR results the inverted curved cross hinge with torsion reinforcements and the inverted cross flexure with torsion reinforcements with 20N contact force, 5N side force.

Rotation of the joint

The Curved Hinge is able to withstand the highest forces parallel to the straightened leaf spring. The total applied force to the joint is equal to the sum of the actuation force F_a and the contact force F_c , see Figure 2. To achieve a favorable load case, the Curved Cross Hinge joint as a whole is rotated by an angle of about 20° to ensure this favorable loading condition over the range of motion.

Torsion Stiffeners

The resistance of the Curved Cross Hinge to torsion due to lateral forces (F_s) is quite low. In fact, the maximum lateral force at 40° deflection angle is just 3N. To prevent large out of plane deflections and to increase load carrying capacity in the transverse direction, triangular torsional reinforcements are used [16]. These triangles allow the main leaf to bend, necessary for flexion, while creating a shape that is stiff in torsion. This is shown in Figure 6. To interfere as little as possible with the rest of the finger, the triangles are placed on the inside of the flexure where possible. The geometry of the triangles is largely bounded by the shape of the flexure, making sure that the reinforcements will not touch the main flexures in all deflected states.

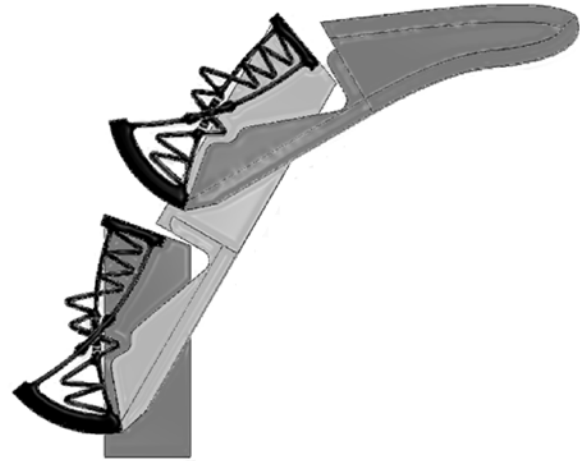


FIGURE 6. Finger design with triangular torsion reinforcements.

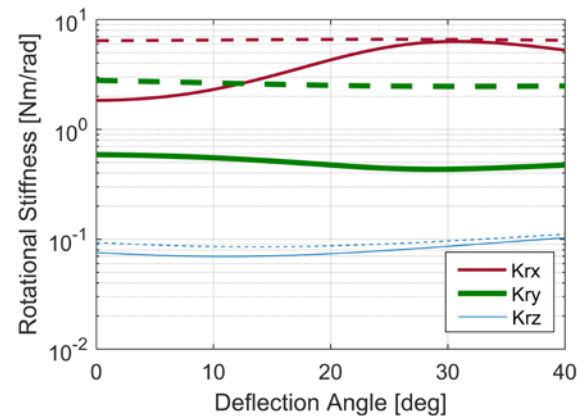


FIGURE 7. Stiffness comparison, reinforced and non-reinforced; Dashed line: Curved Hinge with torsion reinforcements; Solid line: Curved Hinge without torsion reinforcements. See Figure 2 for coordinate system.

In Figure 7 the effect of the torsion reinforcement is shown. An increase in rotational stiffness around the y-axis of a factor 6 is achieved. Additionally the joint is now able to withstand 5N lateral forces, compared to 1.2N without torsion stiffeners. The triangles also give the joint higher and more constant stiffness around the x-axis (K_{rx}). The increase in actuation stiffness (z-axis, K_{rz}) is relatively small so no significantly higher actuation forces are needed.

Overload Protection

Due to the inversion of the leaf springs, the phalanges are crossing. This crossing is conveniently used to create mechanical end stops. The side flanges of the finger prevents the leaves in the joint from excessive twisting.

EXPERIMENTAL VALIDATION

A physical 3D-printed part has been additively manufactured with Selective Laser Sintering (SLS) to test the functionality and verify the obtained grasping/actuation force,. A photograph of the prototype is provided in figure 9.

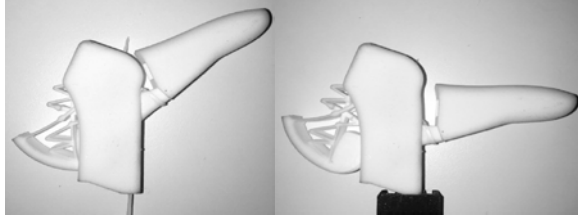


Figure 9. Un-deflected and 40° deflected 3D-printed (SLS) prototype finger.

For validation of the grasping force, the finger is actuated with a tendon with a predefined actuation force and the resulting grasping force is measurement with a force sensor. The experimental setup is pictured in figure 10.

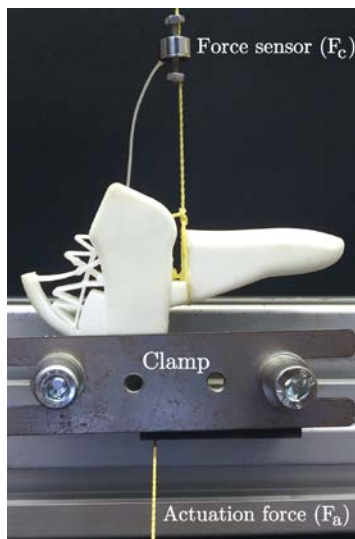


Figure 10. Experimental setup for testing grasping force

The measured actuation and grasping force is provided in figure 10. From these results it can be concluded that the required grasping force of 20N can be obtained without failure/buckling of the flexures. Furthermore, a small offset between the resulting grasping force can be observed under full extension (the user has to push to the fingers to obtain full extension, resulting in initial grasping force of approximately 3N) and full flexion (initial actuation force is required to obtain the required deflection angle).

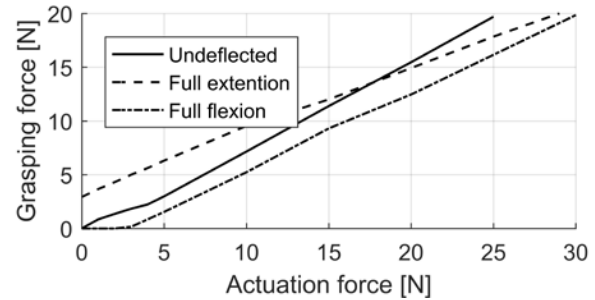


Figure 11. Measured grasping force at undelected state, full extension and full flexion.

CONCLUSION

The presented prosthetic flexure-based finger joint is able to achieve 20N of contact force with an additional 5N out of plane load over the entire 80° range of motion, which is a major improvement over existing prosthetic flexure-based finger designs.

REFERENCES

- [1] M. Tavakoli, A. Sayuk, J. Lourenço, and P. Neto, "Anthropomorphic finger for grasping applications: 3D printed endoskeleton in a soft skin," *Int. J. Adv. Manuf. Technol.*, 2017.
- [2] V. Kalpathy and H.-J. Su, "A 3-Spring Pseudo-Rigid-Body Model for Soft Joints with Significant Elongation Effects A 3-Spring Pseudo-Rigid-Body Model for Soft Joints with Significant Elongation Effects," *J. Mech. Robot.*, 2016.
- [3] L. U. Odhner, L. P. Jentoft, M. R. Claffee, N. Corson, Y. Tenzer, R. R. Ma, M. Buehler, R. Kohout, R. D. Howe, and A. M. Dollar, "A compliant, underactuated hand for robust manipulation," *Int. J. Rob. Res.*, vol. 33, no. 5, pp. 736–752, 2014.
- [4] G. Berselli, F. Parvari Rad, R. Veretchy, and V. Parenti Castelli, "Comparative evaluation of straight and curved beam flexures for selectively compliant mechanisms," 2013 IEEE/ASME Int. Conf. Adv. Intell. Mechatronics Mechatronics Hum. Wellbeing, AIM, 2013.
- [5] B. P. Trease, Y.-M. Moon, and S. Kota, "Design of Large-Displacement Compliant Joints," *J. Mech. Des.*, vol. 127, no. 4, p. 788, 2005.
- [6] D. Brouwer, J. Meijaard, and J. B. Jonker, "Large deflection stiffness analysis of parallel prismatic leaf-spring flexures," *Precis. Eng.*, 2013.

- [7] D. Wiersma, S. E. Boer, R. Aarts, and D. Brouwer, "Design and Performance Optimization of Large Stroke Spatial Flexures," *J. Comput. Nonlinear Dyn.*, vol. 9, no. January 2014, 2013.
- [8] S. Awtar, "Analysis of Flexure Mechanisms in the Intermediate Displacement Range," in *Handb. Compliant Mech.*, L. L. Howell, S. P. Magleby, and B. M. Olsen, Eds. John Wiley & Sons Ltd, 2013.
- [9] G. Berselli, A. Guerra, G. Vassura, and A. O. Andrisano, "An engineering method for comparing selectively compliant joints in robotic structures," *IEEE/ASME Trans. Mechatronics*, 2014.
- [10] L. U. Odhner and A. M. Dollar, "The smooth curvature model: An efficient representation of Euler-Bernoulli flexures as robot joints," *IEEE Trans. Robot.*, vol. 28, no. 4, pp. 761–772, 2012.
- [11] I. M. Bullock, J. Z. Zheng, S. De La Rosa, C. Guertler, and A. M. Dollar, "Grasp frequency and usage in daily household and machine shop tasks," *IEEE Trans. Haptics*, vol. 6, no. 3, pp. 296–308, 2013.
- [12] C. Cipriani, M. Controzzi, and M. Carrozza, "The SmartHand transradial prosthesis," *J. Neuroeng. Rehabil.*, 2011.
- [13] A.D. Astin, 'Finger force capability: measurement and prediction using anthropometric and myoelectric measures', master thesis, Faculty of the Virginia Polytechnic Institute and State University, 1999
- [14] Jonker, J.B. and Meijaard, J.P., 'Spacar – Computer Program for Dynamic Analysis of Flexible Spatial Mechanisms and Manipulators', *Multibody Systems Handbook*, W. Schiehlen (eds.), SpringerVerlag, Berlin, pp. 123-143, 1990.
- [15] Brouwer, D.M., Meijaard, J.P., Jonker, J.B., 'Elastic Element Showing Low Stiffness Loss at Large Deflection', *Proceedings of the 24th annual meeting of the American Society of Precision Engineering*, Monterey, pp. 30-33, 2009.
- [16] M. Naves, D.M. Brouwer, R.G.K.M. Aarts, Building block based spatial topology synthesis method for large stroke flexure hinges, *ASME robotics and mechanisms*, 2017.